Network analysis reveals succession of *Microcystis* genotypes accompanying distinctive microbial modules with recurrent patterns

Seong-Jun Chun [a, b], Yingshun Cui [a], Jay Jung Lee [c], In-Chan Choi [c], Hee-Mock Oh [a, b, **], Chi-Yong Ahn [a, b, *]

[a] *Cell Factory Research Center, Korea Research Institute of Bioscience and Biotechnology (KRIBB), Daejeon 34141, Republic of Korea*
[b] *Department of Environmental Biotechnology, KRIBB School of Biotechnology — Korea University of Science and Technology (UST), Daejeon 34113, Republic of Korea*
[c] *Geum River Environment Research Center, National Institute of Environmental Research, Chungbuk 29027, Republic of Korea*

ABSTRACT

Every member of the ecological community is connected via a network of vital and complex relationships, called the web of life. To elucidate the ecological network and interactions among producers, consumers, and decomposers in the Daechung Reservoir, Korea, during cyanobacterial harmful algal blooms (cyanoHAB), especially those involving *Microcystis*, we investigated the diversity and compositions of the cyanobacterial (16S rRNA gene), including the genotypes of *Microcystis* (*cpcBA*-IGS gene), non-cyanobacterial (16S), and eukaryotic (18S) communities through high-throughput sequencing. *Microcystis* blooms were divided into the Summer Major Bloom and Autumn Minor Bloom with different dominant genotypes of *Microcystis*. Network analysis demonstrated that the modules involved in the different phases of the *Microcystis* blooms were categorized into the Pre-Bloom, Bloom, Post-Bloom, and Non-Bloom Groups at all sampling stations. In addition, the non-cyanobacterial components of each Group were classified, while the same Group showed similarity across all stations, suggesting that *Microcystis* and other microbes were highly interdependent and organized into cyanoHAB-related module units. Importantly, the *Microcystis* genotype-based sub-network uncovered that *Pirellula, Pseudanabaena,* and *Vampirovibrionales* preferred to interact with specific *Microcystis* genotypes in the Summer Major Bloom than with other genotypes in the Autumn Minor Bloom, while the copepod *Skistodiaptomus* exhibited the opposite pattern. In conclusion, the transition patterns of cyanoHAB-related modules and their key components could be crucial in the succession of *Microcystis* genotypes and to enhance the understanding of microbial ecology in an aquatic environment.

© 2019 Elsevier Ltd. All rights reserved.

1. Introduction

Microbes consist of viruses, bacteria, archaea, and eukaryotes that generate diverse ecological relationships in complex ecosystems (Coyte et al., 2015). Through these interactions, the microbes can overcome their weaknesses and revitalize their strengths (Faust and Raes, 2012). In a freshwater ecosystem, a harmful algal bloom is one of the most important environmental issues (Heisler et al., 2008). In particular, the cyanobacteria *Microcystis*, *Dolichospermum* (formerly *Anabaena*), and *Pseudanabaena* form cyanobacterial harmful algal blooms (cyanoHAB) that cause serious problems for both the environment and human health by disrupting food web dynamics, creating hypoxic zones, and producing toxins (Paerl and Otten, 2013). *M. aeruginosa* is one of the most common freshwater cyanoHAB species worldwide, including in South Korea (Srivastava et al., 2015). Since our study area (Daechung Reservoir) exclusively suffers from a *Microcystis* bloom almost every year, including in 2017, cyanoHAB in this study refers only to the *Microcystis* bloom.

The species that cause cyanoHAB do not live alone in aquatic ecosystems but consistently interact with various microorganisms in a variety of ways, ranging from predator-prey to mutualistic interactions. Cyanobacteria can provide a favorable environment for

microbes by producing oxygen and cyanobacteria-derived substances such as extracellular polysaccharides (EPS) (Rossi and De Philippis, 2015). Heterotrophic bacteria can produce bacterial cell-derived substances, such as nutrients and microelements, for cyanobacteria by decomposing organic polymers into small molecules that can be readily used by cyanobacteria (Li et al., 2011; Wang et al., 2016). Grazing effects on cyanobacteria by eukaryotic protists, such as ciliates, copepods, and rotifers, also represent major interrelationships during bloom periods (Dryden and Wright, 1987; Liu et al., 2012). Recently, many studies have revealed a close association between heterotrophic bacteria and cyanobacteria (Liu et al., 2019b; Louati et al., 2015; Niu et al., 2011; Woodhouse et al., 2018). Niu et al. (2011) reported that the bacterial community compositions shifted with fixed patterns during phytoplankton bloom periods, showing that the succession of phytoplankton communities significantly influences the bacterial communities. The interactions between cyanobacteria and bacteria could be based on the degradation of dissolved organic matter and the recycling of nutrients (Louati et al., 2015). In the case of eukaryotes, the co-occurrence patterns among the eukaryotic community are not consistent but vary significantly during the phytoplankton bloom period (Liu et al., 2019a). In addition, the cooperation of rare planktonic eukaryotes contributes to the stability and resilience of the microbial community during cyanoHAB (Xue et al., 2018). These interactions play a crucial role in the algal proliferation and degradation processes in an aquatic ecosystem. Moreover, many researchers have focused on the diversity and composition of *Microcystis* genotypes and found that the temporal variation in them was significantly correlated with nutrient concentrations (Guan et al., 2018). Furthermore, the shift of *Microcystis* genotypes resulted in different microcystin production (Wang et al., 2013). Therefore, revealing the microbial interactions between producers (mainly cyanobacteria), consumers (mainly eukaryotes), and decomposers (mainly heterotrophic bacteria) is important for understanding the hidden underlying mechanisms of cyanoHAB.

Because ecosystems are more complex and diverse than our expectations, the results obtained from the co-culture experiments are not able to precisely reflect the real interactions between bloom-forming species and the surrounding microbes in a complex ecosystem. With an increasing amount of information, such as microbial community data generated by next-generation sequencing and advanced computational techniques, biological association networks are becoming a fundamental tool for the investigation of high-throughput data in biology (Faust and Raes, 2012). The power and usefulness of biological association networks originate from their ability to extract new information from ecological interactions, organizations, keystone organisms (i.e., connectors and hubs), and their responses to environmental variables that can not be revealed by conventional techniques. Among the various network analysis techniques, extended local similarity analysis (eLSA) is one of the most powerful methods for uncovering statistically significant local and even potentially time-delayed association patterns in time-series data beyond conventional correlation analyses (Xia et al., 2011). eLSA has been used to investigate a broad range of microbial interactions in various environments, including soil (Thomas and Cébron, 2016), marine (Chow et al., 2014), and freshwater (Yang et al., 2018). For instance, Yang et al. (2018) revealed that the influence of interspecific associations was greater on the phytoplankton community and ecological network than the extrinsic effects of environmental factors.

To understand the complex interactions between producers, consumers, and decomposers during cyanoHAB, samples were collected weekly from the Daechung Reservoir, Korea, and the diversity and composition of the cyanobacterial, including genotypes of *Microcystis*, non-cyanobacterial and eukaryotic communities were investigated using high-throughput sequencing. To our knowledge, this is the first study to combine these three major components and interpret microbial modular structures during cyanoHAB.

The Daechung Reservoir is a large branch-type reservoir (gross storage capacity of 1490 Mm^3) where serious cyanobacterial blooms have been observed every year since the end of the 1980s (Ahn et al., 2002; Oh et al., 2007; Srivastava et al., 2015). It is the most important water resource in Daejeon city and the Chungcheong Province and supplies water to over 4 million people for drinking, agricultural, and industrial use. In this study, data were combined, including biophysicochemical characteristics and microbial community compositions, and merged into an association network for each sampling site. Then, the transition patterns of major modules were categorized into Group units to understand the complex interactions between producers, consumers, and decomposers during cyanoHAB. Here, the following questions are addressed: "How do non-cyanobacteria bacterial community composition (NC-BCC) and eukaryotic community composition (ECC) vary seasonally with different *Microcystis* genotypes and microcystin congeners at different nutrient concentrations?", "Are there any recurrent modules with a pattern associated with cyanoHAB (cyanoHAB-related modules)?", and finally, "Which groups are key factors in these cyanoHAB-related modules?"

2. Methods

2.1. Sample collection and water quality analysis

Freshwater samples were collected on a weekly basis from 19 June 2017 to 10 October 2017 at the water surface from three sites (Chuso, Hoenam, and Janggye) in the Daechung Reservoir, Korea (Fig. S1), resulting in 16 total time points and 48 total samples. Water temperature, pH, dissolved oxygen (DO), and conductivity were measured at the sampling sites using a multi-parameter water quality probe (6600EDS, YSI, USA) (Tables S1, S2, and S3). Turbidity was measured using an instrument (2100Q, Hach, USA) that analyzed the samples transported to the laboratory. Concentrations of chlorophyll-*a* (chl-*a*), total nitrogen (TN), total dissolved nitrogen (TDN), nitrate, ammonia, total phosphorus (TP), total dissolved phosphorus (TDP), chemical oxygen demand (COD), suspended solids (SS), and total organic carbon (TOC) were determined by the Geum River Environment Research Center according to the Standard Methods for the Examination of Water and Wastewater (APHA, 2005) (Tables S1, S2, and S3). Analyses of geosmin and 2-methylisoborneol (2-MIB) were carried out by a GC-MS system (TSQ 8000 Evo, Thermo, USA) using samples prepared by the HS-SPME (head space solid-phase microextraction) method (Saito et al., 2008). Analyses of microcystins (MCs) and anatoxin were carried out by a UPLC–MS/MS system (Xevo TQ-S, Waters, USA) using samples prepared by ultrasonic destruction of the phytoplankton which was verified by microscopic observation (Oehrle et al., 2010). The algal identification and cell count were performed under a microscope (Nikon ECLIPSE Ti–S, Nikon Corp., Tokyo, Japan). The microscopic images were acquired with a digital camera (DS-Ri2, Nikon Corp., Tokyo, Japan).

2.2. Microbial community composition including bacteria, eukaryotes, and genotypes of Microcystis

For the microbial community analysis, 2-L water samples were collected and stored in a cooler until filtration. Filtration and DNA extraction were processed according to the method described in our previous report (Chun et al., 2019). The bacterial 16S rRNA gene was amplified using a universal bacterial primer set, 341F/805R

(341F: CCTACGGGNGGCWGCAG; 805R: GACTACHVGGGTATC-TAATCC), which targets the V3−V4 region of the 16S rRNA gene (Herlemann et al., 2011). The eukaryotic 18S rRNA gene was amplified using a universal eukaryotic primer set, V8f/1510r (V8f: ATAACAGGTCTGTGATGCCCT; 1510r: CCTTCYGCAGGTTCACCTAC), which targets the V8−V9 region of the 18S rRNA gene (Bradley et al., 2016). To investigate the genotypes of *Microcystis*, the gene sequences of the intergenic spacer (IGS) between *cpcB* and *cpcA* (*cpcBA*-IGS), the phycocyanin locus of the photosynthetic apparatus in cyanobacteria, were selected with a primer set, cpc57F/cpc356R (cpc57F: AACCTATGTAGCTTTAGGAGTACC; cpc356R: CTTAA-GAAACGACCTTGAGAATC) (Kim et al., 2010). This primer set was designed to identify both toxic and non-toxic *Microcystis* geno-types, but not other cyanobacteria, and has been used for *Micro-cystis* genotype analysis (Guan et al., 2018; Wang et al., 2013). PCR amplification, purification, and quantification were performed ac-cording to the method described in our previous report (Chun et al., 2019). MiSeq Version 3 Chemistry (Illumina) was used for paired-end reads sequencing reactions and sequenced using a MiSeq (2 × 300 bp reads) from the Macrogen Corporation (Seoul, South Korea).

The resulting raw sequences of 16S and 18S rRNA genes were processed using Mothur (version 1.39.1) (Schloss et al., 2009), ac-cording to the MiSeq standard operating procedure (accessed date: 5 June 2018, http://www.mothur.org/wiki/MiSeq_SOP) with some modifications (Kozich et al., 2013). Briefly, low-quality sequences were removed from the analysis when they contained ambiguous characters, contained more than two mismatches to the forward primer or one mismatch to the barcode, or were less than 300 bp or more than 500 bp in length. The latest Silva database (release 132) was used to align and classify the sequences (Quast et al., 2013). Furthermore, the TaxAss 16S rRNA database and pipeline were used for NC-BCC classification (Rohwer et al., 2018, accessed 12 October 2019). After classifying the sequences, chloroplast and mitochon-dria sequences were removed from the dataset. Eukaryotic organ-isms have intragenomic variability (generally <1% variation) that can potentially overestimate diversity from 18S rRNA gene surveys (Gong et al., 2013). Therefore, to avoid this problem, a similarity cutoff of 98% was used to assign the same Operational Taxonomic Unit (OTU) for eukaryotes (Behnke et al., 2011), and a 99% cutoff for bacteria (Edgar, 2018). In addition, OTUs that comprised only sin-gletons, doubletons, and tripletons were not subjected to further analyses. Furthermore, the 16S rRNA gene sequence data sets were split into two partitions, the "cyanobacteria" and "non-cyano-bacterial groups" based on the Silva database's phylum classifica-tion of the 16S rRNA gene.

To investigate sequence variants at a single nucleotide in the *cpcBA*-IGS gene, Amplicon Sequence Variants (ASVs) of the *cpcBA*-IGS gene were calculated through DADA2 (version 1.8), according to the pipeline tutorial 1.8 (accessed date: 14 October 2018, https://benjjneb.github.io/dada2/tutorial_1_8.html) in R (Callahan et al., 2016). Each ASV of the *cpcBA*-IGS gene was defined as each different *Microcystis* genotype in this study. The phylogenic tree of *cpcBA*-IGS was constructed using a neighbor-joining (Saitou and Nei, 1987) algorithm in MEGA 6 (Tamura et al., 2013), and the bootstrap values were calculated from 1000 replications. Reference sequences were collected by blasting against the available *cpcBA*-IGS gene sequences from the National Center for Biotechnology Information (NCBI) public database. The sum of the relative abun-dance of the *cpcBA*-IGS gene was normalized to the relative abun-dance of the *Microcystis* OTU for further analysis. The raw sequences and accompanying metadata are available in the Sequence Read Archive (SRA) of the NCBI under the project accession number PRJNA509704.

2.3. Microbial association network and topological features

To investigate the relationships among cyanobacteria, geno-types of *Microcystis*, non-cyanobacterial groups, eukaryotes, and environmental variables, three microbial association networks were constructed for the three sampling sites using eLSA (Xia et al., 2011). Only OTUs that met the following thresholds for each given data set were considered: (1) detected in 30% of samples and (2) a relative proportion of >0.1% for at least one day. *P*-values were estimated using a "mixed" approach. The *Q*-value (false discovery rate) was calculated to estimate the likelihood of false positives. Both *P*- and *Q*-values were calculated using the eLSA command "lsa_compute". Only positive correlations that had both a *P*- and *Q*-value < 0.001 were selected for further analyses. The network was visualized using the open-source software Cytoscape 3.5.1 (Shannon et al., 2003).

Network topological features were calculated using the "Net-workanalyzer" plugin in Cytoscape and R software (package: igraph) (Assenov et al., 2007; Csardi and Nepusz, 2006). Random undirected networks of equal size in terms of the number of nodes and edges were calculated using the Erdős−Rényi model using the Network Randomizer plugin in Cytoscape. The small-world coeffi-cient (SW) is defined as SW = clustering coefficient (C/C$_R$)/char-acteristic path length (L/L$_R$) ($_R$ represents parameters from a random network) (Table 1). To build a sub-network, the three networks were combined into one network, the microbial recur-rent association network (MRAN), according to the method described by Chun et al. (2019), and the sub-network was extracted from MRAN.

2.4. Module calculation, transition patterns of modules, and groups

The modules were identified using the Louvain algorithm in R software (package: igraph) (Csardi and Nepusz, 2006; Blondel et al., 2008). To calculate the transition patterns of the major modules, the relative abundance of OTUs (except environmental parameters, *Microcystis* OTUs, and genotypes) in each module were normalized using feature scaling. After normalization, normalized OTUs in each module were averaged together to calculate the transition patterns of each module (Chun et al., 2019). Then, a dendrogram was con-structed based on the transition patterns of the major modules using Ward's method as implemented in the function "hclust" of the R package (version 3.4.0) (R Core Team, 2017) to separate the major modules into several categories (we defined these categories as Group). Finally, we compared each Group with the relative abundance of *Microcystis* OTU in the total bacterial community to identify the Bloom Group, Post-Bloom Group, Pre-Bloom Group, and Non-Bloom Group.

2.5. Different topological roles of individual nodes and statistical analysis

To identify the topological roles of each node in the microbial network, we calculated within-module degree (Z_i) and among-module connectivity (P_i) (Guimera and Amaral, 2005). According to the threshold values of Z_i and P_i described in Olesen et al. (2007), the nodes were divided into peripherals, module hubs, connectors, and network hubs. All statistical analyses were performed using the R package (version 3.4.0) (R Core Team, 2017). We used non-metric multidimensional scaling (NMDS) analysis with Bray−Curtis dis-tances to ordinate the samples based on their dissimilarity in NC-BCC and ECC using the "metaMDS" function in Vegan (Oksanen et al., 2013). Differences in taxonomic composition among the different bloom periods were tested using PERMANOVA with 999 permutations, using the Vegan function "adonis". The

Table 1
Topological features and statistics of microbial association networks.

	Chuso		Hoenam		Janggye	
	Observed	Random	Observed	Random	Observed	Random
Nodes	448		474		407	
Edges	1629		2294		718	
Average number of neighbours	7.27		9.68		3.43	
Network density	0.016		0.02		0.009	
Diameter	16	6	19	6	13	6
Network heterogeneity	1.09	0.38	1.04	0.34	0.93	0.62
Centralization	0.082	0.014	0.087	0.029	0.044	0.015
Modularity	0.59	0.37	0.59	0.30	0.74	0.53
Average clustering coefficient (C)	0.24	0.013	0.25	0.015	0.14	0.006
Characteristic path length (L)	4.77	3.48	4.38	3.12	6.24	5.61
C/C_r	18.31		16.67		23	
L/L_r	1.37		1.4		1.11	
Small-world coefficient (SW)	13.37		11.87		20.69	

assemblage—environment—major cyanobacterial OTUs relationships were examined by fitting vectors onto the ordination space using the Vegan function "envfit". The significance of the fitted vectors was assessed using a permutation procedure (permutation 999).

3. Results

3.1. Biophysicochemical characteristics

Biophysicochemical characteristics data for each sampling site are shown in Tables S1, S2, and S3. The water temperature increased up to 32.9–33.7 °C on 7 August and decreased to below 25 °C on 10 October during the sampling periods. The concentration of chl-a reached its maximum value of 54.6–74.6 μg/L when the *Microcystis* bloom occurred (Fig. 1A). Both DO and pH increased during the bloom period. Among the nutrients, concentrations of TN ranged from 0.42 to 2.19 mg/L (Fig. 6A), while those of TDN and NO_3–N ranged from 0.34 to 2.13 and 0.22–1.71 mg/L, respectively. The TP ranged from 0.009 to 0.107 mg/L (Fig. 6B). Concentrations of geosmin significantly increased up to 534 ng/L at the Hoenam station during July 10–24. Furthermore, the concentration of MC was approximately three times higher in the bloom period than in the post-bloom period (Fig. 6C). The maximum concentrations of the MC-RR and -LR were 0.34 and 0.24 μg/L, respectively, while that of MC-YR was 0.12 μg/L.

3.2. Cyanobacterial, non-cyanobacterial, and eukaryotic community composition

A total of 3213 OTUs were clustered at 99% similarity for bacteria: 3017 OTUs were assigned to non-cyanobacterial groups and 196 OTUs to *Cyanobacteria*. The proportions of *Cyanobacteria* varied over the sampling stations and period, ranging from 2.7% to 56.1% in the total bacterial community (Fig. 1A). Since the top seven most abundant cyanobacterial OTUs occupied approximately 85% of the total cyanobacterial community, we defined these cyanobacterial OTUs as major cyanobacteria in this study: *Microcystis* (OTU0002), *Cyanobium* (OTU0003 and 0004), *Pseudanabaena* (OTU0005 and OTU0014), *Dolichospermum* (formerly *Anabaena*) (OTU0008), and *Aerosakkonema* (OTU0013). The relative abundance of *Microcystis* (OTU0002) significantly correlated with the cell number of *Microcystis* (Spearman correlation $\rho = 0.882$, $P < 0.0001$, $n = 48$) (Tables S4, S5, and S6). From an OTU perspective, a total of 12 OTUs were assigned to *Microcystis*, and OTU0002 dominated 99.9% of the *Microcystis* relative abundance.

To identify the diversity of the *Microcystis* genotype, genotype analysis was performed for *Microcystis* using DADA2 with the genotypes of the *cpcBA*-IGS gene. A total of 118 genotypes of *Microcystis* were observed, and their transition patterns were clear during the sampling period. Microscopic images also showed the coexistence of several *Microcystis* morphotypes during the sampling period (Fig. S6A). Different *Microcystis* genotypes dominated during different periods: cpc_ASV001, 003, and 004 dominated from the middle of June to late August (defined as Summer Major Bloom), while cpc_ASV002 dominated in September (defined as Autumn Minor Bloom) (Fig. 1B). Since cell concentrations of *Microcystis* during the Summer Major Bloom were much higher than during the Autumn Minor Bloom, the Summer Major Bloom was defined as the *Microcystis* bloom period, the period prior to this as the pre-bloom period, and that after this as the post-bloom period. Therefore, the Autumn Minor Bloom was observed in the post-bloom period. The average cell concentration of *Microcystis* was approximately 110,000 cells ml^{-1} during the bloom period, but 1000 and 7000 cells ml^{-1} in the pre-bloom and post-bloom period, respectively (Tables S4, S5, and S6).

The relative abundance of *Dolichospermum* (OTU0008) and concentration of geosmin were significantly increased together at the Hoenam station from 10 to 24 July (Fig. 1A and Table S2). *Pseudanabaena* appeared simultaneously with *Microcystis* ($R = 0.81$, $P < 0.001$) (Fig. S6B). Microscopic images obtained from the Daechung Reservoir also confirmed the epiphytic characteristic of these two cyanobacterial species (Figs. S6B and D). Furthermore, *Pseudanabaena* OTU was more closely correlated with cpc_ASV006 in all three stations (recurrence = 3/3). In case of *Cyanobium* sp., two OTUs continuously dominated the cyanobacterial population during the sampling period at the Chuso and Janggye stations.

The NC-BCC changed dramatically during the outbreak and decline of the *Microcystis* bloom. At the class level, *Alphaproteobacteria*, *Bacteroidetes*, and *Actinobacteria* dominated in the non-cyanobacteriabacterial communities during the sampling period (Fig. 1C). During the *Microcystis* bloom period, the relative abundances of *Acetobacterales*, *Caulobacterales*, *Chloroflexales*, *Cytophagales*, *Methylacidiphilales*, OPB56, *Pirellulales*, and *Solibacterales* in NC-BCC were significantly higher, compared to the non-bloom period ($P < 0.005$), while the abundance of the LD12 tribe (alfV-A) decreased to 0.04–3.2% from 42.7-51.6% of the NC-BCC in the same period (Fig. S2).

A total of 2126 eukaryotic OTUs were clustered at 98% similarity for eukaryotes. Similar to NC-BCC, the ECC also varied considerably in the *Microcystis* bloom period. The ECCs mainly comprised phytoplankton, copepods, ciliates, and rotifers (Fig. 1D). *Cryptomonadales*, especially *Cryptomonas* and *Teleaulax*, continuously dominated the eukaryotic phytoplankton communities

(12.7 ± 6.2%) throughout the sampling period, while *Chlamydomonadales* (especially *Volvox*) increased temporarily at the Chuso and Janggye stations. However, Cyanobacteria continuously dominated phytoplankton communities (80.0 ± 25.5%) (Tables S4, S5, and S6). Therefore, cyanoHAB, especially those formed by *Microcystis*, was focused on in this study. The abundance of *Calanoida*, a major copepod (21.6 ± 20.1%), increased during the bloom periods (Fig. S3). *Ciliophora*, known as a ciliate, was dominated by the

Spirotrichea (especially *Halteria*, *Rimostrombidium*, and *Strombidium*) and the CONthreeP group (*Colpodea*, *Oligohymenophorea*, *Nassophorea*, *Prostomatea*, *Plagiopylea*, and *Phyllopharyngea*).

Given the large variation in the relative abundance of the NC-BCC and ECC across samples, we analyzed multidimensional scaling to seek environmental (Tables S1, S2, and S3) and biological variables that acted as potential drivers in reshaping the NC-BCC and ECC. After fitting the environmental and biological variables
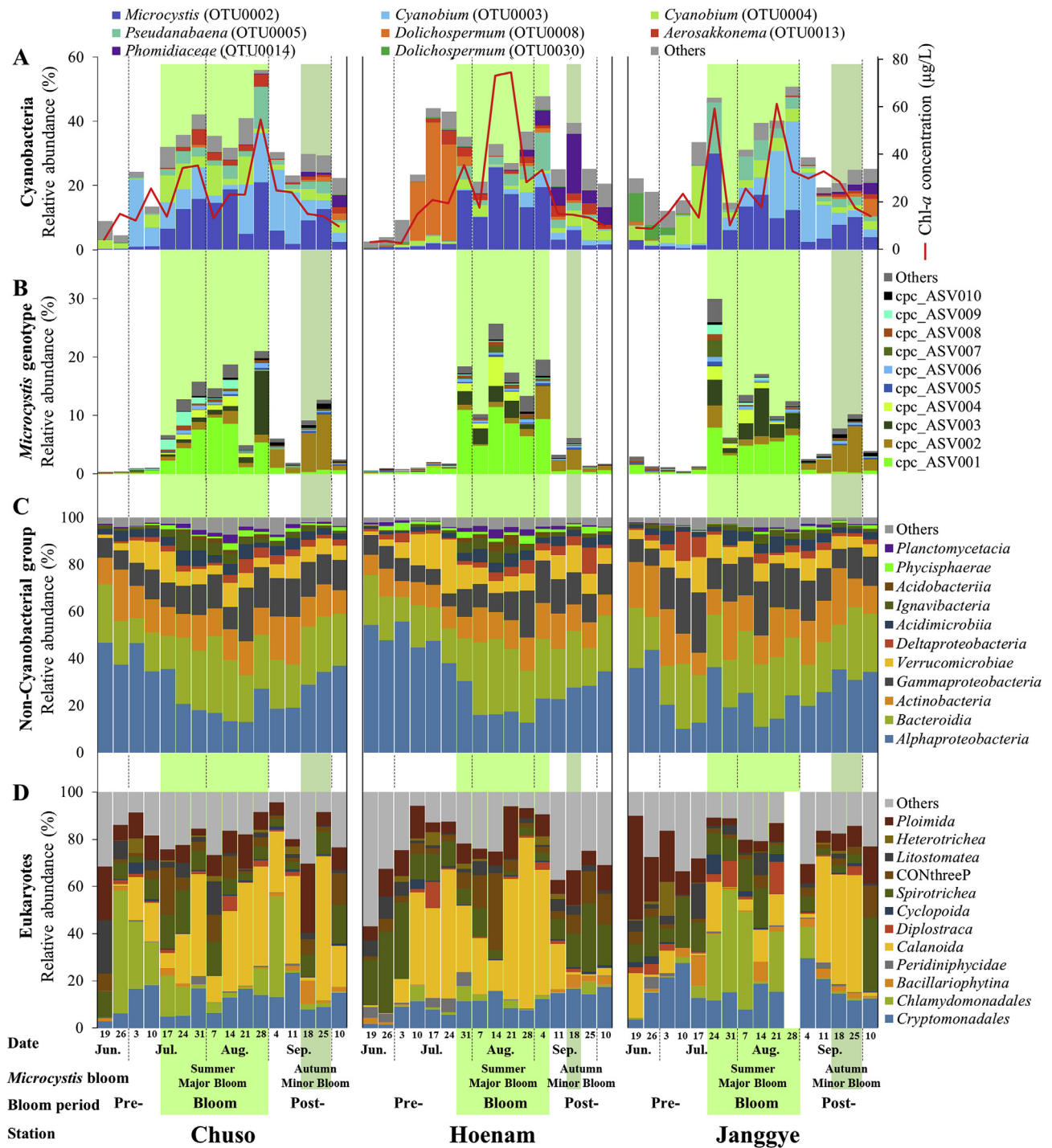

Fig. 1. The relative abundance of (A) major cyanobacterial community structure in the total bacteria community with chl-*a* concentration, (B) *Microcystis* genotypes community structure, (C) non-cyanobacterial community structure, and (D) eukaryotic community structure. The sum of the relative abundance of the *cpcBA*-IGS gene was normalized to the relative abundance of the *Microcystis* OTU. The rectangular green box represents the *Microcystis* bloom period. (For interpretation of the references to color in this figure legend, the reader is referred to the Web version of this article.)

onto the NMDS ordination, we found that pH, cpc_ASV001, COD, *Microcystis* (OTU0002), and cpc_ASV006 were significantly related to the two NMDS axes of the NC-BCC ordination ($r^2 > 0.5$, $P < 0.001$), while temperature, COD, and cpc_ASV001 were significantly related to the two NMDS axes of the ECC ordination ($r^2 > 0.5$, $P < 0.001$) (Fig. S4 and Table S7). The NC-BCC and ECC were segregated into the pre-bloom, bloom, and post-bloom periods (PERMANOVA; NC-BCC, pseudo-$F = 5.28$, DF $= 3$, $P < 0.001$; ECC, pseudo-$F = 2.15$, DF $= 3$, $P < 0.001$).

3.3. Topological features of the networks and modular structure

To construct an association network, 335 bacterial OTUs, 229 eukaryotic OTUs, ten *Microcystis* genotypes, and 19 environmental variables were selected. Three different networks were constructed from different sampling stations using eLSA (Fig. 2). The topological features of the networks are summarized in Table 1. Briefly, each node has an average of 3.43–9.68 links according to the different stations. Modularity was higher compared to their random network. The average clustering coefficient (C, higher values of which indicate communities are well connected among each other) and characteristic path length (L, the average shortest path between all pairs of species) in the three networks were higher than those of their Erdős–Rényi random networks. Accordingly, the SW values (the higher values of which indicate more small-worldliness of the network) were greater than 1, suggesting that these networks have small-world properties. Each association network from the three sampling stations was composed of six to nine major modules, which occupied 77–85% of the total nodes in each association network (Tables 1 and S8).

3.4. Transition patterns of modules and group characteristics

The dendrogram separated the transition patterns of the major modules (cyanoHAB-related modules) into four Groups that were related to the rise and fall of the *Microcystis* bloom (Fig. 3A). The transition patterns of Modules I and V at the Chuso station (C–I and C–V), Module I at the Hoenam station (H–I), and Modules I and IV at the Janggye station (J-I and J-IV) showed similar patterns of the relative abundance of the *Microcystis* OTU, we defined these modules as 'Bloom Group' (Fig. 3E). In contrast, the patterns of Module III at the Chuso station (C-III), Module II at the Hoenam station (H-II), and Module IX at the Janggye station (J-IX) were opposite to the patterns of the Bloom Group (Fig. 3C). These modules were defined as the 'Non-Bloom Group'. The normalized proportions of several modules increased in the post-bloom period (defined as 'Post-Bloom Group') (Fig. 3D), while other modules increased in the pre-bloom period (defined as 'Pre-Bloom Group') (Fig. 3B).

The components of the NC-BCC varied largely in the different Groups but showed a certain consensus among the different stations (Fig. 4B–D), except for the Pre-Bloom Group (Fig. 4A). For example, the alfVIII lineage (*Acetobacterales*), PnecB lineage (*Betaproteobacteriales*), *Cytophagales*, and *Methylacidiphilales* were identified as specific members in the Bloom Group (Fig. 4D). In the case of the ECC, ciliate CONthreeP, mainly *Oligohymenophorea*, were the dominant ciliate in the Bloom Group, while *Chlamydomonadales* was a major group at the Janggye station (Fig. 4H). In the Non-Bloom Group, the LD12 tribe (alfV-A) and *Spirotrichea* were the dominant groups in the NC-BCC and ECC, respectively (Fig. 4B and F). In addition, several OTUs assigned to the acI-A and acI-B lineage (*Frankiales*) were observed in the Non-Bloom Group. Furthermore, the acI-C lineage (*Frankiales*), *Opitutales*, and *Phycisphaerales* were
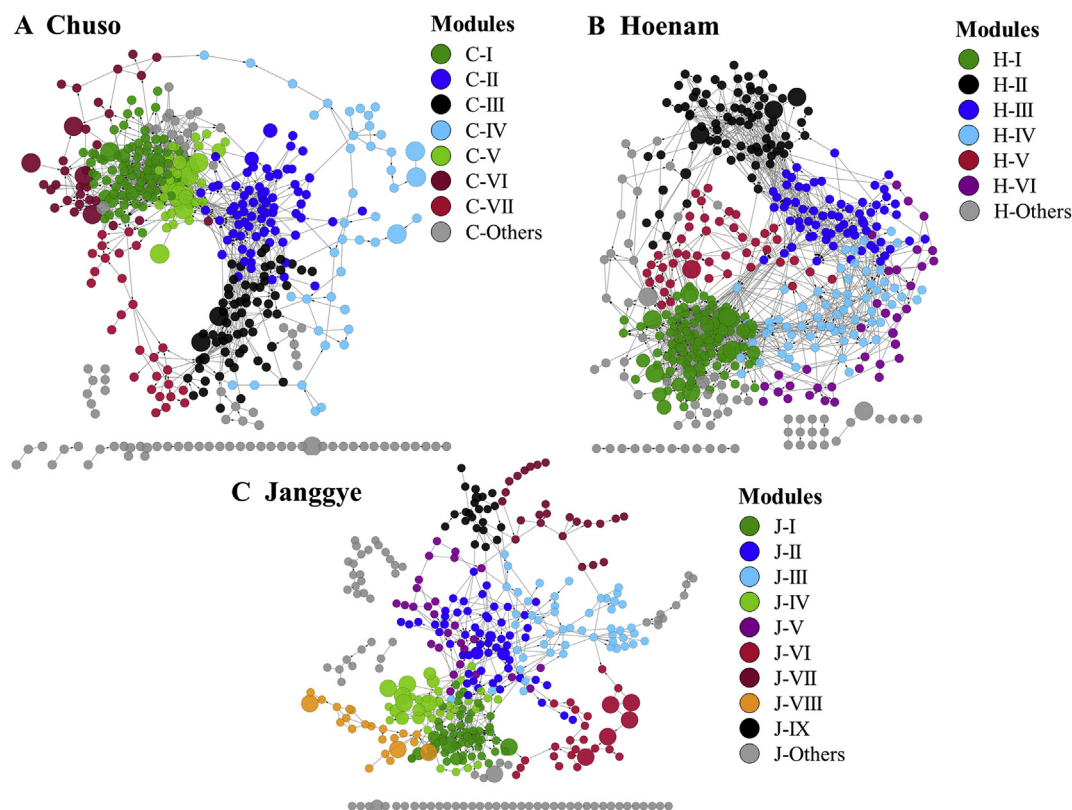

Fig. 2. Microbial association networks at the (A) Chuso station (B) Hoenam station, and (C) Janggye station. The node colors represent major modules. (For interpretation of the references to color in this figure legend, the reader is referred to the Web version of this article.)
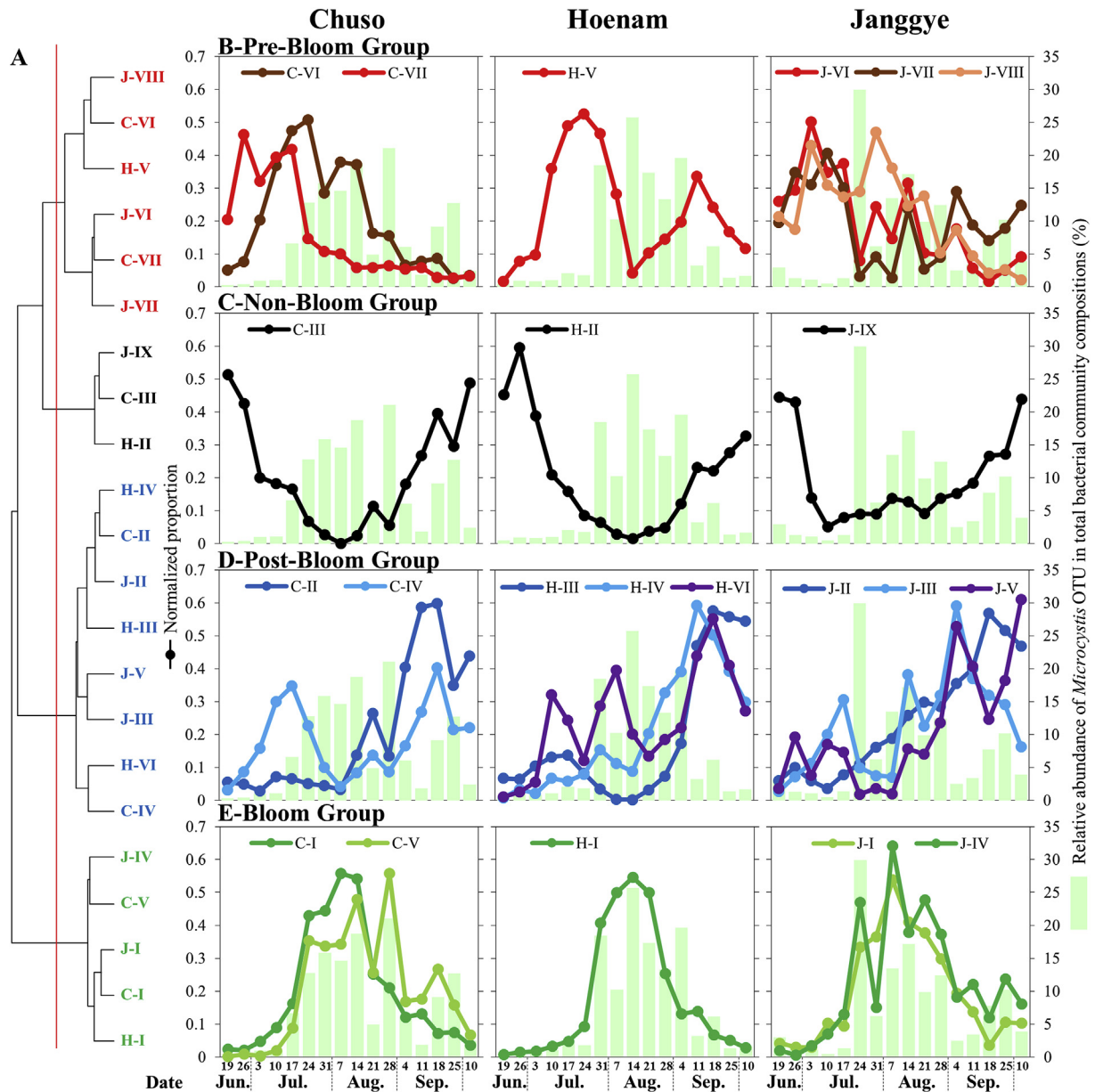
Fig. 3. The transition patterns and classification of major modules with the relative abundance of *Microcystis* OTU in the total bacterial community at the Chuso, Hoenam, and Janggye stations. (A) Dendrogram obtained by hierarchical clustering analysis based on the transition patterns of individual modules, (B) Pre-Bloom Group, (C) Non-Bloom Group, (D) Post-Bloom Group, and (E) Bloom Group.

specific components of the NC-BCC in the Post-Bloom Group (Fig. 4C). The bacI and bacIV lineage (*Chitinophagales*) were found in both the Pre-Bloom Group and Non-Bloom Group. The acI-A lineage was also a dominant group in the Pre-Bloom Group at Hoenam and Janggye stations, while the OPB56, *Chthoniobacterales*, and betIV lineage (*Betaproteobacteriales*) were specific components at the Chuso, Hoenam, and Janggye stations, respectively (Fig. 4A).

3.5. Topological roles and interconnections of microbes for the major cyanobacteria and Microcystis genotypes

To evaluate the potential importance of individual nodes during the *Microcystis* bloom period, Z_i and P_i were calculated. Almost all nodes (>97%) were assigned to peripheral nodes, but only 1% of the nodes were module hubs and connectors, respectively (Fig. S5). Large proportions of connectors (40%) and module hubs (20%) were directly linked to *Microcystis* OTU or genotypes.

To explore the detailed relationships between the major cyanobacteria and other microbes, the major cyanobacterial OTUs and their directly linked (path length = 1) microbes were selected to form a sub-network (Fig. 5A). Major cyanobacteria were also tightly coupled with one another, such as *Microcystis* and *Pseudanabaena*, in all three stations (recurrence = 3/3). In addition, several microbes (e.g., *Microscillaceae*, *Burkholderiaceae*, SM2D12 (*Rickettsiales*), etc.) were directly linked to more than one major cyanobacteria. Among them, four OTUs were assigned to connectors: *Labrys*, acI-C2 lineage, *Vorticella*, and unidentified *Burkholderiaceae*. The *Microscillaceae* OTU was assigned to a module hub. However, the 16S rRNA gene sequence similarities of the *Microscillaceae* OTUs were lower than 92% with the type species of the *Microscillaceae*. Notably, six OTUs, which were assigned to the *Microscillaceae*, *Vampirovibrionales*, *Burkholderiaceae*, and NS9 marine group, were directly linked to *Microcystis* more than twice in three different networks (recurrence ≥ 2/3). The sub-network
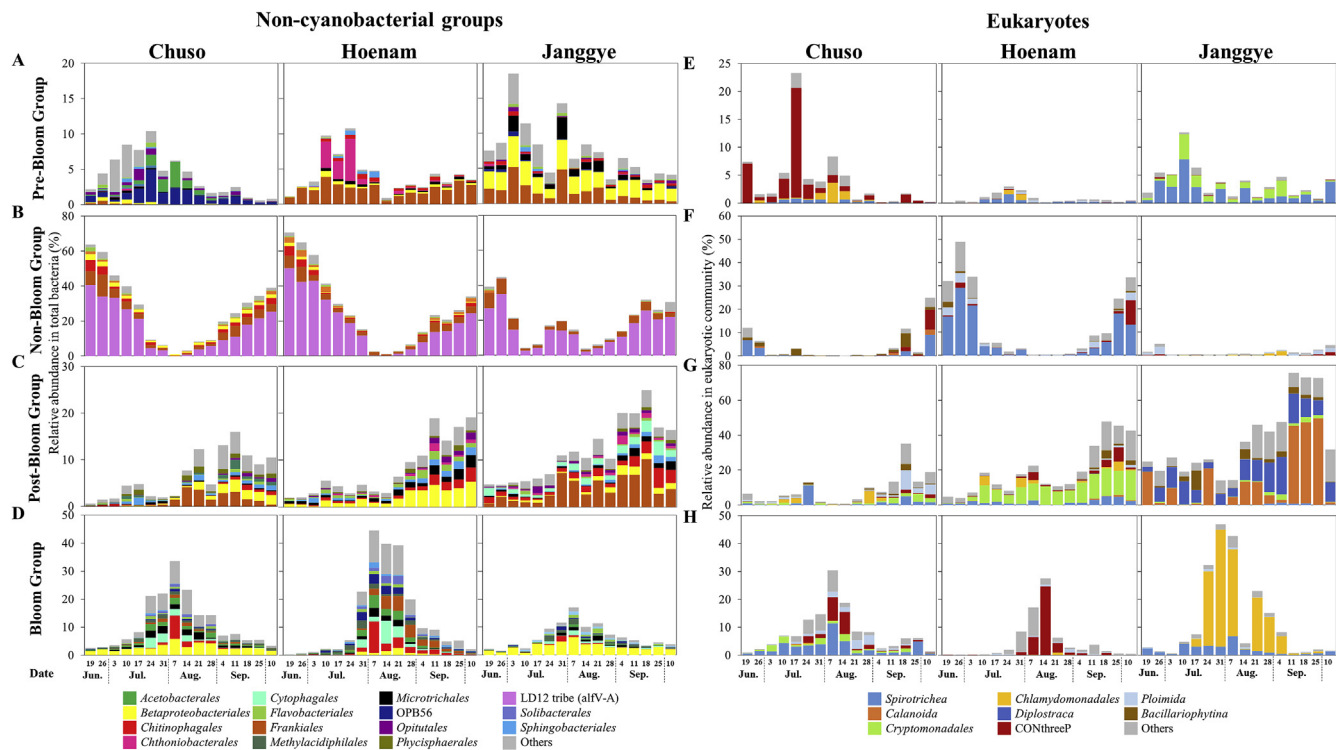
Fig. 4. Average relative abundance of (A–D) non-cyanobacterial groups and (E–H) eukaryotes. (A and E) Pre-Bloom Group, (B and F) Non-Bloom Group, (C and G) Post-Bloom Group, and (D and H) Bloom Group.

showed that MC-LR and −RR were connected to the *Microcystis* OTU (Fig. 5A).

Furthermore, to investigate the microbial interactions between the genotypes of *Microcystis* and other microbes, another sub-network with microbes that were directly connected to the major *Microcystis* genotypes was constructed (Fig. 5B). The sub-network showed highly dynamic interconnections (Table S9). Among them, eight OTUs were assigned to the connectors, and three OTUs were assigned to module hubs. cpc_ASV001, cpc_ASV003, cpc_ASV004, and cpc_ASV006, major genotypes in the Summer Major Bloom, were tightly connected with each other (recurrence ≥ 2/3) and clustered into the Summer Major Bloom cluster with several microbes, while cpc_ASV002 and cpc_ASV009, major genotypes in the Autumn Minor Bloom cluster, were coupled solidly and constructed a relatively small network compared to the Summer Major Bloom cluster. *Microscillaceae*, *Roseomonas*, alfVIII, and *Burkholderiaceae* appeared repeatedly in the Summer Major Bloom cluster. In detail, *Pirella* and *Blastopirellula* were closely correlated with the *Microcystis* OTU and the specific genotypes of *Microcystis*. Copepod *Skistodiaptomus* was directly correlated to cpc_ASV002. *Lacibacter* and the CL500-29 marine group were connected with cpc_ASV001 in a delay correlation (recurrence = 2/3, 1-week lag). Unclassified *Vampirovibrionales* (OTU0066) was correlated to the *Microcystis* OTU repeatedly (recurrence = 2/3) and several dominant *Microcystis* genotypes in the Summer Major Bloom (Fig. 5). The sub-network showed that MC-LR, −RR, and -YR were involved in the Summer Major Bloom cluster rather than the Autumn Minor Bloom cluster (Fig. 5B).

3.6. Interconnections between the nutrients, microcystins, and microbes

To explore the microbial responses against the different nutrients and MC concentrations, a sub-network was extracted that consisted of direct links (path length = 1) between microbes and these parameters (Fig. 6D). No direct links were observed within nutrient concentrations and *Microcystis* genotypes (Fig. 6D). However, TP was connected to several bacterial OTUs, including connector bacteria, which were linked with *Microcystis* genotypes. Among these bacteria, the bacII-A lineage (*Flavobacterium*) connected both the TDP and *Microcystis* genotype. Nitrogen compounds formed an independent network with the bacI lineage (*Chitinophagales*), acI-A, and acI-B lineage OTUs. MCs correlated with a wide variety of microbes, including the alphaI cluster (*Rhizobiales*), *Burkholderiaceae*, Flavo-A1 (*Flavobacteriales*), *Oligoflexaceae*, and *Silanimonas* (*Xanthomonadaceae*) (Fig. 6D). Most of the microbes correlated with MCs were also correlated with *Microcystis* genotypes. In addition, *Bradymonadales* and OPB56 showed delayed correlations with MCs.

4. Discussion

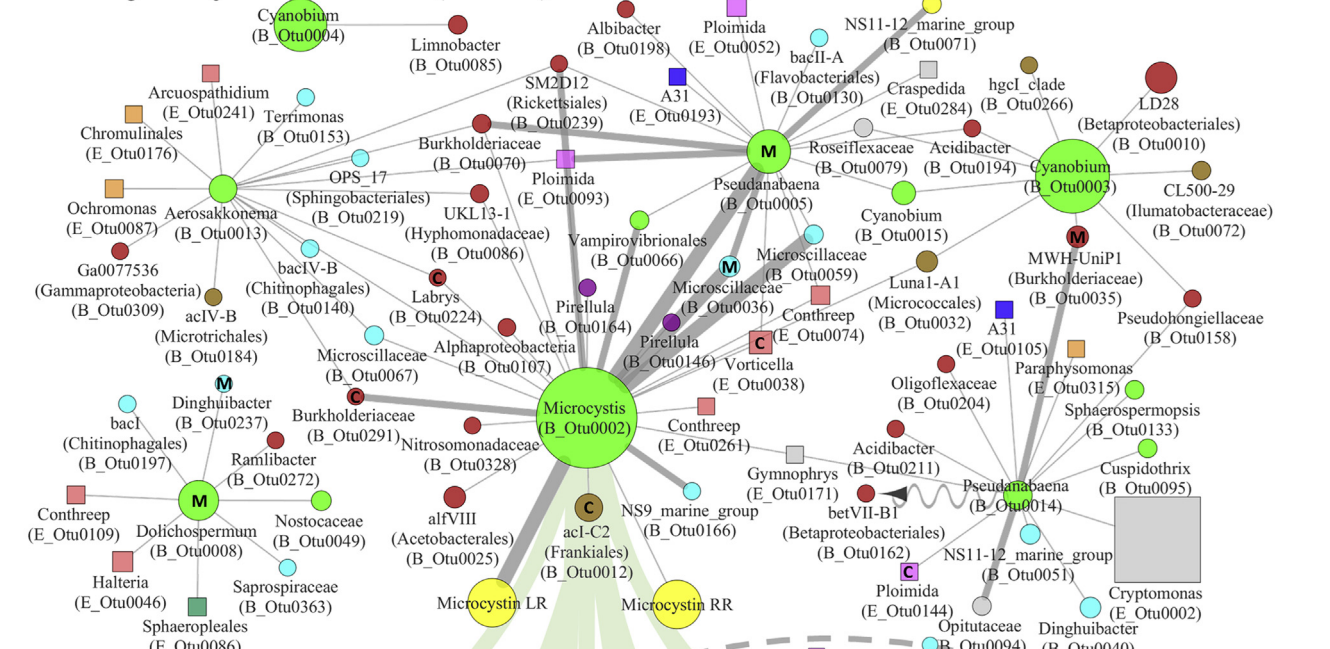### 4.1. Cyanobacterial community dynamics and biophysicochemical characteristics

Microcystis blooms occur annually in the Daechung Reservoir (Srivastava et al., 2015; Ahn et al., 2011; Oh et al., 2001). Many studies have revealed that multiple ecotypes of *Microcystis* coexist in environments by focusing on the intra-specific levels and their diverse physiological characteristics (Guan et al., 2018; Wang et al., 2013; Wilson et al., 2005; Yoshida et al., 2008). This study is the first to perform a genotype analysis of the *Microcystis* genotypes based on the *cpcBA*-IGS genes using next-generation sequencing. Our results show that only one *Microcystis* OTU (16S rRNA gene-based community data) was predominant at the sampling sites, but there were several different *Microcystis* genotypes that dominated at different times (Figs. S6A and C). Furthermore, two major genotypes of *Microcystis* were identical (100% similarity) to clones

analyzed in our previous study that were obtained from the same study sites (Fig. S7) (Kim et al., 2006), indicating that the dominant genotypes did not change in the Daechung Reservoir.

Water temperature is an important environmental factor for the alternating succession of *Microcystis* species (Imai et al., 2008). The Summer Major Bloom and Autumn Minor Bloom appeared from July to August (29.7 ± 1.8 °C) and in September (26.5 ± 0.7 °C), respectively. Bozarth et al. (2010) also observed two types of bloom peaks in mid-July and early September, which accompanied the *Microcystis* population turnover in the Copco Reservoir in the USA. Therefore, the optimum temperatures for different *Microcystis* genotypes could be different and seem to cause a shift in the major
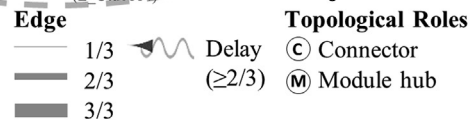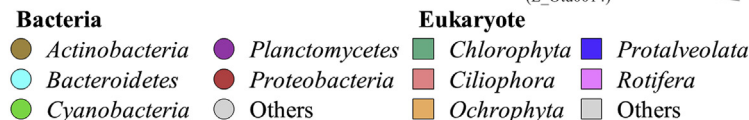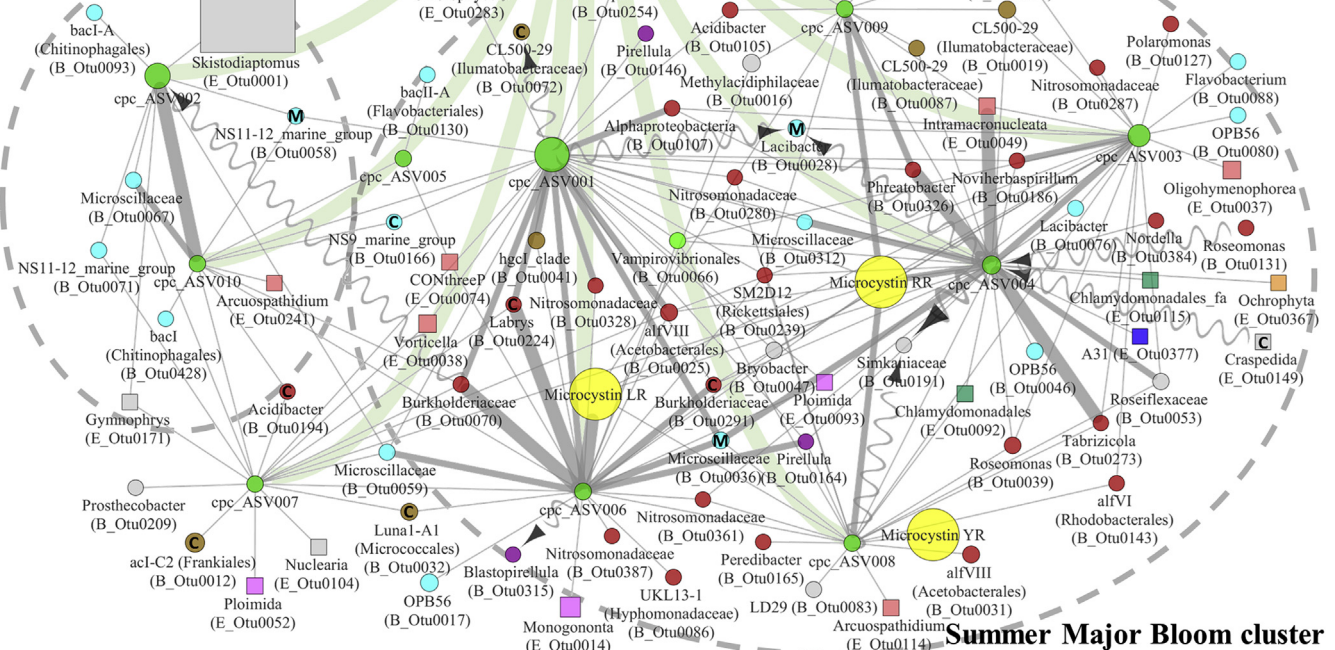

Fig. 5. The sub-network of (A) major cyanobacterial OTUs and (B) *Microcystis* genotypes. The node size represents average relative abundance. The arrow represents a delayed correlation.
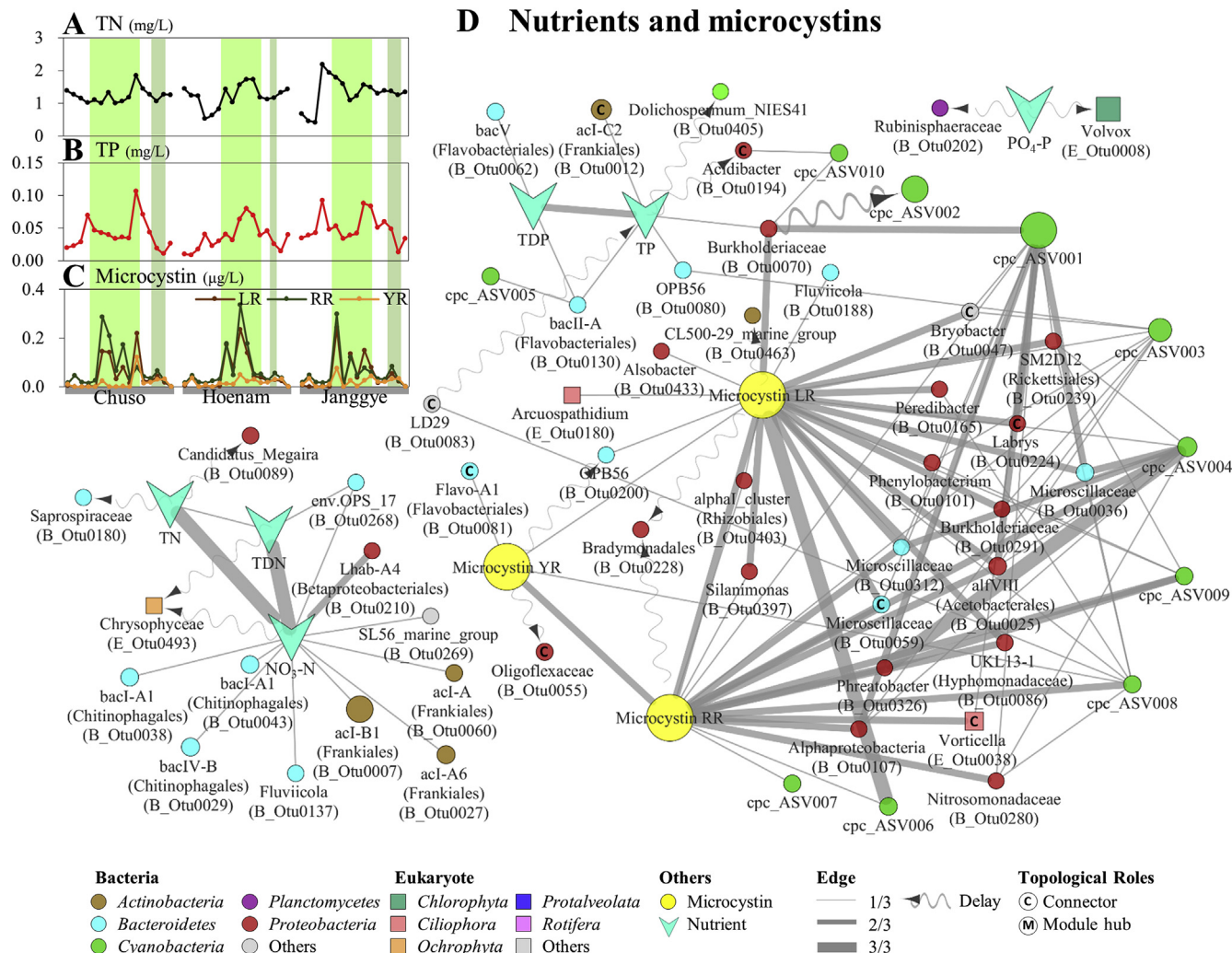
Fig. 6. Concentrations of (A) TN, (B) TP, and (C) microcystins. (D) The sub-network of nutrients and microcystins with microbes. The node size represents average relative abundance. The arrow represents a delayed correlation.

genotypes. In addition, the co-occurrence patterns of minor genotypes also differed across the bloom period, suggesting that the physiological characteristics of these genotypes were different, depending on the bloom stages.

Strains of *Microcystis* can be divided into two categories: toxic and non-toxic *Microcystis* based on their ability to produce cyclic heptapeptide hepatotoxins, called microcystins (MCs). Three variants of MC-LR, −RR, and -YR are the most abundant in *Microcystis* (Fastner et al., 1999). The results of this study suggest that the major genotypes of the Summer Major Bloom could be assigned to toxic *Microcystis* (especially cpc_ASV004, 006, 008, 009), while the major genotypes of the Autumn Minor Bloom (especially cpc_ASV002) could be non-toxic *Microcystis*. Genotype cpc_ASV006 correlated more strongly to MC-LR than to MC-RR or MC-YR, implying that each *Microcystis* genotype has a different production potential for specific MC congeners (Figs. 5B and 6D). As the Summer Major Bloom occurred, high levels of MCs were maintained (Fig. 6C), which would naturally lead to an increase in MC-degrading microorganisms. Some of the species from *Burkholderiaceae*, *Rhizobiales*, and *Xanthomonadaceae* have been reported as MC-degrading bacteria (Rapala et al., 2005; Yang et al., 2014; Zhu et al., 2016). In addition, *Silanimonas* has been isolated in toxic *Microcystis* cultures (Chun et al., 2017). However, most of the bacteria that correlated

with MC defy isolation from the environment. Therefore, the results from this study may be used as a hint for discovering MC-degrading microorganisms and finding novel MC-degradation mechanisms. Furthermore, ozonation, chlorination, and oxidation-based water treatment processes have been described to remove MC (Hitzfeld et al., 2000). Most technologies face challenges for scaling-up, including high costs and optimum efficiencies (Hitzfeld et al., 2000). Since the results of this study showed that MCs were mainly linked with the Summer Major Bloom, the MC removal technology should primarily be more focused here.

Microcystis colonies could provide favorable microenvironments for other cyanobacteria and heterotrophic bacteria (Brunberg, 1999). *Pseudanabaena mucicola* could be epiphytic on *Microcystis* colonies and co-occurred during the bloom periods (Agha et al., 2016; Vasconcelos et al., 2011). Agha et al. (2016) revealed that interactions between *Pseudanabaena* and *Microcystis* are dynamic (neutral to antagonistic) and depend on different *Microcystis* strains. The results of this study also suggested that the relationship between *Pseudanabaena* and *Microcystis* could be genotype-specific.

The order *Vampirovibrionales* consists of non-photosynthetic *Cyanobacteria* (class *Melainabacteria*), which are known as predatory bacteria (Soo et al., 2015). *Vampirovibrio chlorellavorus* adheres

to the surface of green alga *Chlorella vulgaris* by specific attachment structures and destroys its prey. Parasites are dependent on their hosts, but negative correlations are not found often at daily to weekly timescales due to relatively low mortality (Berdjeb et al., 2018). The recurrent correlation (recurrence = 2/3) between *Vampirovibrionales* OTU and *Microcystis* suggests that the unclassified strain of *Vampirovibrionales* could be one of the important predatory bacteria of *Microcystis*.

4.2. Microbial interactions within the cyanoHAB-related modules and group

The effect of protists, zooplankton, predatory bacteria, and viruses are a major factor that contributes to mortality and the succession of *Microcystis* (Harke et al., 2016). A large amount of *Microcystis* biomass could be lysed by predator-prey interactions or cellular senescence during the bloom phase. *Cytophagales* is already known as an obligate parasite of freshwater *Cyanobacteria* (Daft and Stewart, 1971), and the unclassified *Vampirovibrionales* (OTU0066) was suggested as the predatory bacteria of *Microcystis* in this study. Previous studies have shown that ciliate, especially *Oligohymenophorea*, had a strong ability to graze the cells of *Microcystis* (Dryden and Wright, 1987; Liu et al., 2012). These groups were found in the Bloom Group and were presumed to mediate predator-prey interactions. Wu and Hahn (2006) suggested that the biomass of phytoplankton could influence the succession of the PnecB lineage. The relative abundance of PnecB bacteria did not correlate with *Microcystis* in this study, even though PnecB bacteria was one of the dominant groups in the Bloom Group. This result suggests that the PnecB lineage could interact with *Microcystis*-related microbes, but not with *Microcystis* directly.

The Non-Bloom Group showed an opposite pattern compared to the Bloom Group (Fig. 3). The major components of the Non-Bloom Group were similar across the stations, and the LD12 tribe (alfV-A), the freshwater sibling of the marine SAR11 clade, was the most dominant group (Fig. 4B). However, little is known regarding the ecophysiological properties of the LD12 tribe. The genomic characteristics of freshwater LD12 revealed that it has an aerobic, chemoorganoheterotrophic lifestyle, thriving in oligotrophic media with simple carbon compounds, and it likely depends on reduced organosulfur compounds and ammonium as its sulfur and nitrogen sources, respectively (Henson et al., 2018). A higher *Microcystis* cell density could accompany a higher concentration of organic matters (high TOC and COD) released by *Microcystis* itself, or by bacteria that degrade *Microcystis*-derived photosynthates resulting in a more eutrophic condition. Therefore, it was inadequate for the LD12 tribe to dominate during the bloom period.

The Post-Bloom Group consisted of at least two modules at each station (Fig. 3D). As major components of the Post-Bloom Group (Fig. 4C), the BacII-A lineage (*Flavobacteriales*) is known as an organic scavenger and degrader of polymers, such as cellulose and chitin (Kirchman, 2002), and high proportions of *Flavobacteria* appear during or after a period of high productivity in eutrophic lakes (Eiler and Bertilsson, 2007; Newton et al., 2011). Consistent with our results, Berry et al. (2017) also reported that the acI-A and acI-B lineages decreased during *Microcystis*-dominant cyanoHAB in Lake Erie, while acI-C increased. Phylogenetically, acI-A and acI-B lineages were closer to each other, compared with the acI-C lineage (Ghylin et al., 2014). In addition, acI-C isolates shared 70−74% of the genomic sequence with several acI-A isolates (Kang et al., 2017). They reported that the acI-C lineage had different genomic characteristics, such as carbon metabolism and nucleotide biosynthesis, compared with the acI-A lineage. It was assumed that these genomic features of the acI lineage could be the underlying reason

for the niche partitioning of this group during the bloom period.

Unlike other groups, the Pre-Bloom Group showed a significant difference in the components between the stations (Fig. 4A). The origins of the water at the Chuso and Janggye stations (main stream) are different, and the Hoenam station is affected by merged water flow from the Chuso and Janggye areas (Fig. S1), which could be one of the reasons for the microbial differences in the Pre-Bloom Group. In addition, the Pre-Bloom Group was also coupled with different *Cyanobacteria*. For instance, the H−V module showed a similar trend with the proliferation of *Dolichospermum* in July, prior to the *Microcystis* bloom (Figs. 1A and 3B). *Chthoniobacterales* dominated the H−V module, suggesting that a specific group of *Chthoniobacterales* could interact with *Dolichospermum* (Fig. 4A). These results suggest that the Pre-Bloom Group is mainly affected by site-specific environments and the proliferation of other cyanobacteria.

Seasonal succession of distinct sets of microbes, i.e., microbial modules, had important roles in the proliferation, maintenance, and degradation of *Microcystis* in this study. A modular organization of species interactions would benefit the dynamic stability of the communities (Grilli et al., 2016). Therefore, they could be presumed to perform ecological functions by working together as a microbial module unit, which could not be done alone.

4.3. Detailed interactions between cyanobacteria and microbes

Pirellula is a free-living bacterium but is also attached to filamentous algae and cyanobacteria by a holdfast (Clum et al., 2009), suggesting that this bacterial group could attach strongly to the surface of *Microcystis* and mediate the coordination of microbial interactions in the phycosphere. Uncultured *Microscillaceae* OTUs were also repeatedly correlated to the *Microcystis* OTU and genotypes, implying a tight interaction. Therefore, further studies should be carried out to isolate these groups and investigate the interaction mechanisms between them and *Microcystis*.

The sub-network of the *Microcystis* genotypes was more complex than the sub-network of the major *Cyanobacteria*. For instance, although the *Vampirovibrionales*, *Pirellula*, *Blastopirellula*, and *Roseomonas* OTUs were connected to the *Microcystis* OTU, these OTUs were connected only to the genotypes of *Microcystis* in the Summer Major Bloom rather than in the Autumn Minor Bloom (Fig. 5B). In contrast, the copepod *Skistodiaptomus* (E_OTU0001) was connected to the Autumn Minor Bloom cluster rather than the Summer Major Bloom cluster, indicating that grazing by copepod *Skistodiaptomus* could be one of the reasons for the short and small proliferation of *Microcystis* during the post-bloom period. The differentiation between the Summer Major Bloom and Autumn Minor Bloom could be explained by the different microbial interconnections within the microbial network. Therefore, the *Microcystis* genotype sub-network could provide a new perspective for a more detailed and precise understanding of the microbial interactions during the *Microcystis* bloom.

Module hubs are responsible for the interactions within the module, while connectors are responsible for the interactions between modules. Previous works have indicated that the damage to module hubs and connectors might cause a collapse of the module and even a disintegration of the global network structure (Guimera and Amaral, 2005; Olesen et al., 2007). Around 100 microbes were assigned to the Bloom Group, but only around 40 microbes connected to *Microcystis* at each station. Approximately 10% of the OTUs, which were directly linked with the *Microcystis* genotypes or OTU, were assigned to connectors or module hubs (Fig. 5). It suggests that *Microcystis* could cooperate with the microbes included in the Bloom Group, primarily through an indirect connection between the connector/module hub microbes and other microbes. For

instance, the connector bacterium *Labrys* was linked to two major *Microcystis* genotypes in the Bloom Group. The genus *Labrys* has been isolated from different environments, such as freshwater, rhizosphere, root nodules, and sediment (Nguyen et al., 2015). Recently, Passari et al. (2016) isolated *Labrys* sp. from the endophytic bacterial community of a plant. Endophytic bacteria colonize within a plant, usually exchanging nutrition with the host and also protecting the host against pathogens by producing a variety of lytic enzymes. It suggests that this connector bacterium could have a similar role as endophytic bacteria in the mucilage of *Microcystis* during the bloom periods.

Importantly, some OTUs, repeatedly linked to *Microcystis* in this study, showed >99% similarity with those found in other aquatic ecosystems where *Microcystis* causes algal blooms (Table S10). The occurrence of the same bacteria not only in the Daechung Reservoir but also in other countries suggests that the *Microcystis* bloom requires common bacteria, firmly connected in an identical module unit. Therefore, it was concluded that cyanoHAB-associated NC-BCC are considerably conserved across the world, and they could be fundamental biological elements for the rise and fall of the *Microcystis* bloom.

5. Conclusion

To our knowledge, this is the first study on microbial modular structures that includes the genotypes of *Microcystis*, non-cyanobacterial groups, and eukaryotes, using eLSA-based network analysis. Next-generation sequencing and genotype analysis revealed that *Microcystis*, a major primary producer, consisted of diverse genotypes during different phases of the bloom, and they interacted with various microbes. *Microcystis* blooms were divided into Summer Major Bloom and Autumn Minor Bloom with different toxin concentration and different dominant genotypes of *Microcystis*. The differentiation between the Summer Major Bloom and Autumn Minor Bloom could be explained by the temperature and the different microbial interconnections within the microbial network. Moreover, reliable and repeated cyanoHAB-related modules were identified by investigating the interrelationship within the microbial food web in a eutrophic reservoir during the *Microcystis* bloom. CyanoHAB-related modules were categorized into the Pre-Bloom, Bloom, Post-Bloom, and Non-Bloom Groups, mainly consisting of non-cyanobacterial groups. These microbes had key roles in the formation, maintenance, and decline of the *Microcystis* bloom. In particular, the alfVIII (*Acetobacterales*), PnecB (*Betaproteobacteriales*), BacII-A (*Flavobacteriales*), and acI-C (*Frankiales*) lineages might be involved in mutualistic interactions, while *Vampirovibrionales, Cytophagales*, and *Oligohymenophorea* might be involved in interactions such as parasitism or predation. Overall, the succession of the *Microcystis* genotypes was found to be regulated by both bottom-up and top-down controls in terms of cyanoHAB-related modules. Therefore, the diversity of the *Microcystis* genotype and cyanoHAB-related modules provides the fundamental basis for understanding the biological mechanisms behind the cyanoHAB.

Declaration of competing interest

The authors declare that they have no known competing financial interests or personal relationships that could have appeared to influence the work reported in this paper.

Acknowledgments

Appendix A. Supplementary data

Supplementary data to this article can be found online at https://doi.org/10.1016/j.watres.2019.115326.

References

Agha, R., del Mar Labrador, M., de los Ríos, A., Quesada, A., 2016. Selectivity and detrimental effects of epiphytic *Pseudanabaena* on *Microcystis* colonies. Hydrobiologia 777 (1), 139–148.

Ahn, C.-Y., Chung, A.-S., Oh, H.-M., 2002. Rainfall, phycocyanin, and N: P ratios related to cyanobacterial blooms in a Korean large reservoir. Hydrobiologia 474 (1–3), 117–124.

Ahn, C.Y., Oh, H.M., Park, Y.S., 2011. Evaluation of environmental factors on cyanobacterial bloom in eutrophic reservoir using artificial neural networks. J. Phycol. 47 (3), 495–504.

APHA, 2005. Standard Methods for the Examination of Water and Wastewater, twenty-first ed. American Public Health Association/American Water Works Association/Water Environment Federation, Washington, DC, USA.

Assenov, Y., Ramírez, F., Schelhorn, S.-E., Lengauer, T., Albrecht, M., 2007. Computing topological parameters of biological networks. Bioinformatics 24 (2), 282–284.

Behnke, A., Engel, M., Christen, R., Nebel, M., Klein, R.R., Stoeck, T., 2011. Depicting more accurate pictures of protistan community complexity using pyrosequencing of hypervariable SSU rRNA gene regions. Environ. Microbiol. 13 (2), 340–349.

Berdjeb, L., Parada, A., Needham, D.M., Fuhrman, J.A., 2018. Short-term dynamics and interactions of marine protist communities during the spring–summer transition. ISME J. 12, 1907–1917.

Berry, M.A., Davis, T.W., Cory, R.M., Duhaime, M.B., Johengen, T.H., et al., 2017. Cyanobacterial harmful algal blooms are a biological disturbance to Western Lake Erie bacterial communities. Environ. Microbiol. 19 (3), 1149–1162.

Blondel, V.D., Guillaume, J.L., Lambiotte, R., Lefebvre, E., 2008. Fast unfolding of communities in large networks. J. Stat. Mech. Theory Exp. 10, P10008.

Bozarth, C.S., Schwartz, A.D., Shepardson, J.W., Colwell, F.S., Dreher, T.W., 2010. Population turnover in a *Microcystis* bloom results in predominantly non-toxigenic variants late in the season. Appl. Environ. Microbiol. 76 (15), 5207–5213.

Bradley, I.M., Pinto, A.J., Guest, J.S., 2016. Design and evaluation of Illumina MiSeq compatible primers for the 18S rRNA gene for improved characterization of mixed microalgal communities. Appl. Environ. Microbiol. 82, 5878–5891.

Brunberg, A.K., 1999. Contribution of bacteria in the mucilage of *Microcystis* spp.(Cyanobacteria) to benthic and pelagic bacterial production in a hyper-eutrophic lake. FEMS Microbiol. Ecol. 29 (1), 13–22.

Callahan, B.J., McMurdie, P.J., Rosen, M.J., Han, A.W., Johnson, A.J.A., et al., 2016. DADA2: high-resolution sample inference from Illumina amplicon data. Nat. Methods 13 (7), 581–583.

Chow, C.-E.T., Kim, D.Y., Sachdeva, R., Caron, D.A., Fuhrman, J.A., 2014. Top-down controls on bacterial community structure: microbial network analysis of bacteria, T4-like viruses and protists. ISME J. 8 (4), 816–829.

Chun, S.-J., Cui, Y., Ko, S.R., Lee, H.G., Oh, H.M., et al., 2017. *Silanimonas algicola* sp. nov., isolated from laboratory culture of a bloom-forming cyanobacterium, *Microcystis*. Int. J. Syst. Evol. Microbiol. 67 (9), 3274–3278.

Chun, S.-J., Cui, Y., Lee, C.S., Cho, A.R., Baek, K., et al., 2019. Characterization of distinct cyanoHABs-related modules in microbial recurrent association network. Front. Microbiol. 10, 1637.

Clum, A., Tindall, B.J., Sikorski, J., Ivanova, N., Mavrommatis, K., et al., 2009. Complete genome sequence of *Pirellula staleyi* type strain (ATCC 27377). Stand. Genomic Sci. 1 (3), 308.

Coyte, K.Z., Schluter, J., Foster, K.R., 2015. The ecology of the microbiome: networks, competition, and stability. Science 350 (6261), 663–666.

Csardi, G., Nepusz, T., 2006. The igraph software package for complex network research. J. Inter. Complex Syst. 1695 (5), 1–9.

Daft, M., Stewart, W., 1971. Bacterial pathogens of freshwater blue-green algae. New Phytol. 70 (5), 819–829.

Dryden, R., Wright, S., 1987. Predation of cyanobacteria by protozoa. Can. J. Microbiol. 33 (6), 471–482.

Edgar, R.C., 2018. Updating the 97% identity threshold for 16S ribosomal RNA OTUs. Bioinformatics 34 (14), 2371–2375.

Eiler, A., Bertilsson, S., 2007. *Flavobacteria* blooms in four eutrophic lakes: linking population dynamics of freshwater bacterioplankton to resource availability. Appl. Environ. Microbiol. 73 (11), 3511–3518.

Fastner, J., Erhard, M., Carmichael, W., Sun, F., Rinehart, K., et al., 1999. Characterization and diversity of microcystins in natural blooms and strains of the genera *Microcystis* and *Planktothrix* from German freshwaters. Arch. Hydrobiol. 1452, 147–163.

Faust, K., Raes, J., 2012. Microbial interactions: from networks to models. Nat. Rev. Microbiol. 10 (8), 538.

Ghylin, T.W., Garcia, S.L., Moya, F., Oyserman, B.O., Schwientek, P., et al., 2014. Comparative single-cell genomics reveals potential ecological niches for the freshwater acI Actinobacteria lineage. ISME J. 8 (12), 2503–2516.

Gong, J., Dong, J., Liu, X., Massana, R., 2013. Extremely high copy numbers and polymorphisms of the rDNA operon estimated from single cell analysis of oligotrich and peritrich ciliates. Protist 164 (3), 369–379.

Grilli, J., Rogers, T., Allesina, S., 2016. Modularity and stability in ecological communities. Nat. Commun. 7, 12031.

Guan, D.-X., Wang, X., Xu, H., Chen, L., Li, P., et al., 2018. Temporal and spatial distribution of Microcystis biomass and genotype in bloom areas of Lake Taihu. Chemosphere 209, 730–738.

Guimera, R., Amaral, L.A.N., 2005. Functional cartography of complex metabolic networks. Nature 433 (7028), 895–900.

Harke, M.J., Steffen, M.M., Gobler, C.J., Otten, T.G., Wilhelm, S.W., et al., 2016. A review of the global ecology, genomics, and biogeography of the toxic cyanobacterium, Microcystis spp. Harmful Algae 54, 4–20.

Heisler, J., Glibert, P.M., Burkholder, J.M., Anderson, D.M., Cochlan, W., et al., 2008. Eutrophication and harmful algal blooms: a scientific consensus. Harmful Algae 8 (1), 3–13.

Henson, M.W., Lanclos, V.C., Faircloth, B.C., Thrash, J.C., 2018. Cultivation and genomics of the first freshwater SAR11 (LD12) isolate. ISME J. 12, 1846–1860.

Herlemann, D.P., Labrenz, M., Jürgens, K., Bertilsson, S., Waniek, J.J., et al., 2011. Transitions in bacterial communities along the 2000 km salinity gradient of the Baltic Sea. ISME J. 5 (10), 1571–1579.

Hitzfeld, B.C., Höger, S.J., Dietrich, D.R., 2000. Cyanobacterial toxins: removal during drinking water treatment, and human risk assessment. Environ. Health Perspect. 108, 113–122.

Imai, H., Chang, K.-H., Kusaba, M., Nakano, S.-i., 2008. Temperature-dependent dominance of Microcystis (Cyanophyceae) species: M. aeruginosa and M. wesenbergii. J. Plankton Res. 31 (2), 171–178.

Kang, I., Kim, S., Islam, M.R., Cho, J.C., 2017. The first complete genome sequences of the acI lineage, the most abundant freshwater Actinobacteria, obtained by whole-genome-amplification of dilution-to-extinction cultures. Sci. Rep. 7, 42252.

Kim, S.-G., Joung, S.-H., Ahn, C.-Y., Ko, S.-R., Boo, S.M., et al., 2010. Annual variation of Microcystis genotypes and their potential toxicity in water and sediment from a eutrophic reservoir. FEMS Microbiol. Ecol. 74 (1), 93–102.

Kim, S.-G., Rhee, S.-K., Ahn, C.-Y., Ko, S.-R., Choi, G.-G., et al., 2006. Determination of cyanobacterial diversity during algal blooms in Daechung Reservoir, Korea, on the basis of cpcBA intergenic spacer region analysis. Appl. Environ. Microbiol. 72 (5), 3252–3258.

Kirchman, D.L., 2002. The ecology of Cytophaga–Flavobacteria in aquatic environments. FEMS Microbiol. Ecol. 39 (2), 91–100.

Kozich, J.J., Westcott, S.L., Baxter, N.T., Highlander, S.K., Schloss, P.D., 2013. Development of a dual-index sequencing strategy and curation pipeline for analyzing amplicon sequence data on the MiSeq Illumina sequencing platform. Appl. Environ. Microbiol. 79 (17), 5112–5120.

Li, H., Xing, P., Chen, M., Bian, Y., Wu, Q.L., 2011. Short-term bacterial community composition dynamics in response to accumulation and breakdown of Microcystis blooms. Water Res. 45 (4), 1702–1710.

Liu, L., Peng, Y.F., Zou, W.B., Yang, X.Y., Pan, X.J., et al., 2012. Isolation and characterization of Microcystis-grazing Protozoa P1 from lake Dianchi. Adv. Mater. Res. 518, 400–405.

Liu, L., Chen, H., Liu, M., Yang, J.R., Xiao, P., et al., 2019a. Response of the eukaryotic plankton community to the cyanobacterial biomass cycle over 6 years in two subtropical reservoirs. ISME J. 13, 2196–2208.

Liu, M., Liu, L., Chen, H., Yu, Z., Yang, J.R., et al., 2019b. Community dynamics of free-living and particle-attached bacteria following a reservoir Microcystis bloom. Sci. Total Environ. 660, 501–511.

Louati, I., Pascault, N., Debroas, D., Bernard, C., Humbert, J.-F., et al., 2015. Structural diversity of bacterial communities associated with bloom-forming freshwater cyanobacteria differs according to the cyanobacterial genus. PLoS One 10 (11), e0140614.

Newton, R.J., Jones, S.E., Eiler, A., McMahon, K.D., Bertilsson, S., 2011. A guide to the natural history of freshwater lake bacteria. Microbiol. Mol. Biol. Rev. 75 (1), 14–49.

Nguyen, N.-L., Kim, Y.-J., Hoang, V.-A., Kang, J.-P., Wang, C., et al., 2015. Labrys soli sp. nov., isolated from the rhizosphere of ginseng. Int. J. Syst. Evol. Microbiol. 65 (11), 3913–3919.

Niu, Y., Shen, H., Chen, J., Xie, P., Yang, X., et al., 2011. Phytoplankton community succession shaping bacterioplankton community composition in Lake Taihu, China. Water Res. 45 (14), 4169–4182.

Oehrle, S.A., Southwell, B., Westrick, J., 2010. Detection of various freshwater cyanobacterial toxins using ultra-performance liquid chromatography tandem mass spectrometry. Toxicon 55 (5), 965–972.

Oh, H.-M., Ahn, C.-Y., Lee, J.-W., Chon, T.-S., Choi, K.H., et al., 2007. Community patterning and identification of predominant factors in algal bloom in Daechung Reservoir (Korea) using artificial neural networks. Ecol. Model. 203 (1–2), 109–118.

Oh, H.-M., Lee, S.J., Kim, J.-H., Kim, H.-S., Yoon, B.-D., 2001. Seasonal variation and indirect monitoring of microcystin concentrations in Daechung Reservoir, Korea. Appl. Environ. Microbiol. 67 (4), 1484–1489.

Oksanen, J., Blanchet, F.G., Kindt, R., Legendre, P., Minchin, P.R., et al., 2013. Package

'vegan'. Community ecology package. version 2 (9), 1–295.

Olesen, J.M., Bascompte, J., Dupont, Y.L., Jordano, P., 2007. The modularity of pollination networks. Proc. Natl. Acad. Sci. USA 104 (50), 19891–19896.

Paerl, H.W., Otten, T.G., 2013. Harmful cyanobacterial blooms: causes, consequences, and controls. Microb. Ecol. 65 (4), 995–1010.

Passari, A.K., Mishra, V.K., Leo, V.V., Gupta, V.K., Singh, B.P., 2016. Phytohormone production endowed with antagonistic potential and plant growth promoting abilities of culturable endophytic bacteria isolated from Clerodendrum colebrookianum Walp. Microbiol. Res. 193, 57–73.

Quast, C., Pruesse, E., Yilmaz, P., Gerken, J., Schweer, T., et al., 2013. The SILVA ribosomal RNA gene database project: improved data processing and web-based tools. Opens external link in new window. Nucleic Acids Res. 41 (D1), 590–596.

R Core Team, 2017. R: A Language and Environment for Statistical Computing. R Foundation for Statistical Computing, Vienna, Austria. URL. https://www.R-project.org/.

Rapala, J., Berg, K.A., Lyra, C., Niemi, R.M., Manz, et al., 2005. Paucibacter toxinivorans gen. nov., sp. nov., a bacterium that degrades cyclic cyanobacterial hepatotoxins microcystins and nodularin. Int. J. Syst. Evol. Microbiol. 55 (4), 1563–1568.

Rohwer, R.R., Hamilton, J.J., Newton, R.J., McMahon, K.D., 2018. TaxAss: leveraging a custom freshwater database achieves fine-scale taxonomic resolution. mSphere 3 (5) e00327-18.

Rossi, F., De Philippis, R., 2015. Role of cyanobacterial exopolysaccharides in phototrophic biofilms and in complex microbial mats. Life 5 (2), 1218–1238.

Saito, K., Okamura, K., Kataoka, H., 2008. Determination of musty odorants, 2-methylisoborneol and geosmin, in environmental water by headspace solid-phase microextraction and gas chromatography–mass spectrometry. J. Chromatogr. A 1186 (1–2), 434–437.

Saitou, N., Nei, M., 1987. The neighbor-joining method: a new method for reconstructing phylogenetic trees. Mol. Biol. Evol. 4 (4), 406–425.

Schloss, P.D., Westcott, S.L., Ryabin, T., Hall, J.R., Hartmann, M., et al., 2009. Introducing mothur: open-source, platform-independent, community-supported software for describing and comparing microbial communities. Appl. Environ. Microbiol. 75 (23), 7537–7541.

Shannon, P., Markiel, A., Ozier, O., Baliga, N.S., Wang, J.T., et al., 2003. Cytoscape: a software environment for integrated models of biomolecular interaction networks. Genome Res. 13 (11), 2498–2504.

Soo, R.M., Woodcroft, B.J., Parks, D.H., Tyson, G.W., Hugenholtz, P., 2015. Back from the dead; the curious tale of the predatory cyanobacterium Vampirovibrio chlorellavorus. PeerJ 3, e968.

Srivastava, A., Ahn, C.-Y., Asthana, R.K., Lee, H.-G., Oh, H.-M., 2015. Status, alert system, and prediction of cyanobacterial bloom in South Korea. BioMed Res. Int. 8, 2015.

Tamura, K., Stecher, G., Peterson, D., Filipski, A., Kumar, S., 2013. MEGA6: molecular evolutionary genetics analysis version 6.0. Mol. Biol. Evol. 30 (12), 2725–2729.

Thomas, F., Cébron, A., 2016. Short-term rhizosphere effect on available carbon sources, phenanthrene degradation, and active microbiome in an aged-contaminated industrial soil. Front. Microbiol. 7, 92.

Vasconcelos, V., Morais, J., Vale, M., 2011. Microcystins and cyanobacteria trends in a 14 year monitoring of a temperate eutrophic reservoir (Aguieira, Portugal). J. Environ. Monit. 13 (3), 668–672.

Wang, W., Shen, H., Shi, P., Chen, J., Ni, L., et al., 2016. Experimental evidence for the role of heterotrophic bacteria in the formation of Microcystis colonies. J. Appl. Phycol. 28 (2), 1111–1123.

Wang, X., Sun, M., Xie, M., Liu, M., Luo, L., et al., 2013. Differences in microcystin production and genotype composition among Microcystis colonies of different sizes in Lake Taihu. Water Res. 47 (15), 5659–5669.

Wilson, A.E., Sarnelle, O., Neilan, B.A., Salmon, T.P., Gehringer, M.M., et al., 2005. Genetic variation of the bloom-forming cyanobacterium Microcystis aeruginosa within and among lakes: implications for harmful algal blooms. Appl. Environ. Microbiol. 71 (10), 6126–6133.

Woodhouse, J.N., Ziegler, J., Grossart, H.-P., Neilan, B.A., 2018. Cyanobacterial community composition and bacteria-bacteria interactions promote the stable occurrence of particle-associated bacteria. Front. Microbiol. 9, 777.

Wu, Q.L., Hahn, M.W., 2006. High predictability of the seasonal dynamics of a species-like Polynucleobacter population in a freshwater lake. Environ. Microbiol. 8 (9), 1660–1666.

Xia, L.C., Steele, J.A., Cram, J.A., Cardon, Z.G., Simmons, S.L., et al., 2011. Extended local similarity analysis (eLSA) of microbial community and other time series data with replicates. BMC Syst. Biol. 5 (Suppl. 2), S15.

Xue, Y., Chen, H., Yang, J.R., Liu, M., Huang, B., et al., 2018. Distinct patterns and processes of abundant and rare eukaryotic plankton communities following a reservoir cyanobacterial bloom. ISME J. 12, 2263–2277.

Yang, F., Zhou, Y., Yin, L., Zhu, G., Liang, G., Pu, Y., 2014. Microcystin-degrading activity of an indigenous bacterial strain Stenotrophomonas acidaminiphila MC-LTH2 isolated from Lake Taihu. PLoS One 9 (1), e86216.

Yang, W., Zheng, Z., Zheng, C., Lu, K., Ding, D., et al., 2018. Temporal variations in a phytoplankton community in a subtropical reservoir: an interplay of extrinsic and intrinsic community effects. Sci. Total Environ. 612, 720–727.

Yoshida, M., Yoshida, T., Satomi, M., Takashima, Y., Hosoda, N., et al., 2008. Intraspecific phenotypic and genotypic variation in toxic cyanobacterial Microcystis strains. J. Appl. Microbiol. 105 (2), 407–415.

Zhu, X., Shen, Y., Chen, X., Hu, Y.O., Xiang, H., et al., 2016. Biodegradation mechanism of microcystin-LR by a novel isolate of Rhizobium sp. TH and the evolutionary origin of the mlrA gene. Int. Biodeterior. Biodegrad. 115, 17–25.